

Scene Summarization: Clustering Scene Videos into Spatially Diverse Frames

Chao Chen¹, Mingzhi Zhu^{1,*}, Ankush Pratap Singh^{1,*}, Yu Yan¹, Felix Juefei-Xu¹, Chen Feng^{1,†}
¹New York University

Abstract

We propose scene summarization as a new video-based scene understanding task. It aims to summarize a long video walkthrough of a scene into a small set of frames that are spatially diverse in the scene, which has many important applications, such as in surveillance, real estate, and robotics. It stems from video summarization but focuses on long and continuous videos from moving cameras, instead of user-edited fragmented video clips that are more commonly studied in existing video summarization works. Our solution to this task is a two-stage self-supervised pipeline named SceneSum. Its first stage uses clustering to segment the video sequence. Our key idea is to combine visual place recognition (VPR) into this clustering process to promote spatial diversity. Its second stage needs to select a representative keyframe from each cluster as the summary while respecting resource constraints such as memory and disk space limits. Additionally, if the ground truth image trajectory is available, our method can be easily augmented with a supervised loss to enhance the clustering and keyframe selection. Extensive experiments on both real-world and simulated datasets show our method outperforms common video summarization baselines by 50%.

1. Introduction

A scene summary represented by a set of images can capture the unique features of a scene and is often required for surveillance, real estate applications like Zillow and GoogleMap because it provides a concise and visually appealing overview of a property. People can quickly assess the space, layout, and overall ambiance, helping them perceive the environment without having to go through an extensive list of details or physically visit the location.

In this work, we present scene summarization, as a new task at the intersection of robotics, computer vision, and multimedia analysis. Its core objective is to tackle the complex task of condensing a long sequence of *scene videos* into a concise set of keyframe images. This process gains

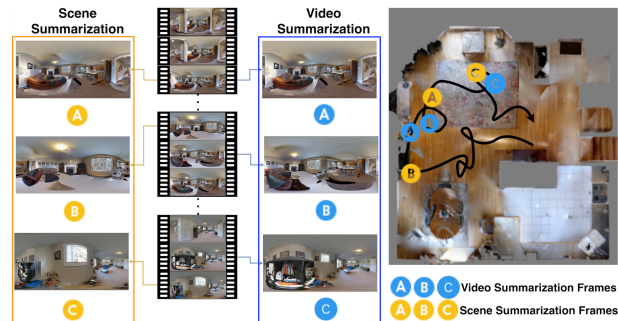


Figure 1. A visual comparison between Scene Summarization and Video Summarization: the orange box shows frames selected by scene summarization, while the blue box shows those by video summarization. The right side shows the trajectory of the camera and the floorplan, with blue/orange dots representing video/scene summarization frames respectively. While the input video is identical, scene summarization promotes *spatial* diversity in the summarized frames, unlike video summarization that may select frames in close spatial proximity (e.g., frame A and B).

particular importance when autonomous robots continually explore and capture *redundant* images of the same environments. In such scenarios, scene summarization enables robots to distinguish, condense, and concisely describe the important visual aspects of the settings they encounter, similar to the principles of video summarization.

However, it is essential to note that scene summarization differs from video summarization in several key ways, primarily in terms of *temporal*, *color*, and *spatial* characteristics. Classic video summarization typically involves compressing video clips based on factors like color distribution or temporal distribution, resulting in temporal discontinuity due to artistic edit. In contrast, scene summarization associates each image with a geographical coordinate, primarily focusing on capturing spatial diversity. Fig. 1 illustrates that the video summarization lacks spatial diversity, resulting in *summarized* frames in close spatial proximity.

An intuitive approach to addressing the scene summarization task involves adopting video summarization techniques. There have been conventional techniques, such as a color-based scene change detection python library PySceneDetect [36], and contemporary deep learning approaches like DR-DSN [55] and CA-SUM [5] which aims

*Equal contribution

†The corresponding author is Chen Feng cfeng@nyu.edu

to condense extensive video content while preserving essential elements. Although suitable for certain contexts, these approaches prove suboptimal for the task of scene summarization. Scene summarization highlights cohesive visual and spatial data, contrasting with existing video summarization methods primarily designed for user-edited and plot-oriented videos. These video summarization methods are not optimized to exploit this inherent coherence. The lack of efficient ways to conduct scene summarization underscores the need for innovative techniques that condense frames in space to achieve the quality of scene summaries.

Our innovation resides prominently within the keyframe selection and ground truth supervision. In contrast to conventional practices that often rely on centroid-based [10] or color histogram-driven [12] techniques for keyframe identification, our approach can retrieve K keyframes from K large-sized clusters without taking into account the memory issue. In summary, the primary contributions of this paper can be summarized as follows:

- We propose the scene summarization task with a specific emphasis on enhancing the spatial diversity of keyframes from scene videos, aiming to deliver more concise and spatially diverse video summaries.
- We introduce the two-stage framework SceneSum, where the first stage involves utilizing clustering to segment a long trajectory into multiple clusters. In the second stage, we employ an autoencoder-decoder structure and contrastive learning loss to generate spatially diverse keyframes within scenes. Additionally, our framework offers the flexibility to incorporate ground truth trajectories for supervising the keyframe selection process.
- We conduct an ablation study, demonstrating that Visual Place Recognition (VPR) features for clustering outperforms traditional image features in the context of scene summarization tasks. Additionally, for large clusters, we devise a cluster sampling process that ensures the global feature of the cluster is sufficiently representative while mitigating GPU memory limitation.
- Our approach demonstrates superior performance in the context of scene summarization, greatly surpassing the efficacy of common video summarization methodologies.

2. Related Work

Classic video summarization. A range of classic techniques has emerged, falling into categories such as clustering-based, change detection-based, and sparse-dictionary-based methods. Within clustering-based approaches, some studies have specifically focused on utilizing color histograms [10, 12, 16, 35, 43]. For instance, VSUMM [10] utilizes K-means clustering, designating each cluster centroid as a keyframe. Meanwhile, STIMO [16] employs the Farthest Point-First (FPF) technique to analyze the color distribution of each frame, dy-

namically creating video storyboards. Change detection-based methods measure the complexity of the sequence in terms of changes in the visual content [11, 12, 20, 31, 40]. Gianluigi and Raimondo [20] introduce a method for choosing representative key frames utilizing various frame descriptors. In contrast, VSUKFE [12] relies on inter-frame discrepancies computed from RGB color channel correlation, color histogram, and moments of inertia. Lastly, one of the proposed techniques uses sparse modeling for representative selection through convex optimization, as described in [14].

Supervised summarization. Deep learning based video summarization leverages advanced neural network architectures (CNN [8, 13, 38], attention [15, 23, 24, 30, 33], GAN [4, 26, 27, 34, 48]) to automatically extract salient information from videos. Among those, supervised approaches normally rely on human annotations of keyframes within a video. HSA-RNN [53] is one typical hierarchical structure-adaptive RNN model that focuses on the temporal dependency of video frames [23, 24, 49, 53]. In contrast, there are several works [8, 13, 22] focusing on the spatial-temporal structure of video frames. Additionally, GAN [4, 26, 27, 34, 48] is also actively used in supervised video summarization task to fool the discriminator when seeing the machine and human-generated summaries.

Self-supervised video summarization. Within the realm of self-supervised techniques [5, 27, 34, 47, 51], several prominent methods have emerged, including adversarial learning based [4, 27, 34, 37, 48], reinforcement learning based [45, 54, 55], motion based [52] approaches. In the domain of adversarial learning, SUM-GAN [34, 48] combines an LSTM-based key-frame selector with a Variational Auto-Encoder (VAE) and a trainable Discriminator. Comparably, reinforcement learning approaches target designed summary properties. For instance, DSN [55] assigns a probability to each video frame, indicating the likelihood of selecting that frame. It then utilizes these probability distributions to make frame selections, ultimately generating video summaries. Lastly, motion-based approaches [52] focus on the key motion of important visual objects using stacked sparse LSTM auto-encoders.

SLAM-based summarization. Video summarization built on top of SLAM relies on estimating the pose of each frame using SLAM techniques and subsequently selecting keyframes based on these estimated poses. In outdoor environments [32, 41, 50], Zhang *et al.* [50] utilize GPS to predict a trajectory and identify popular places or hotspots, aiming for extensive coverage with minimal redundancy. However, the urban canyon effect can lead to some popular spots being missed by GPS coverage. In contrast, indoor scenarios [9, 46] present an even more challenging situation, as there is no GPS coverage available. Attempting to predict poses using SLAM may result in error accumulation

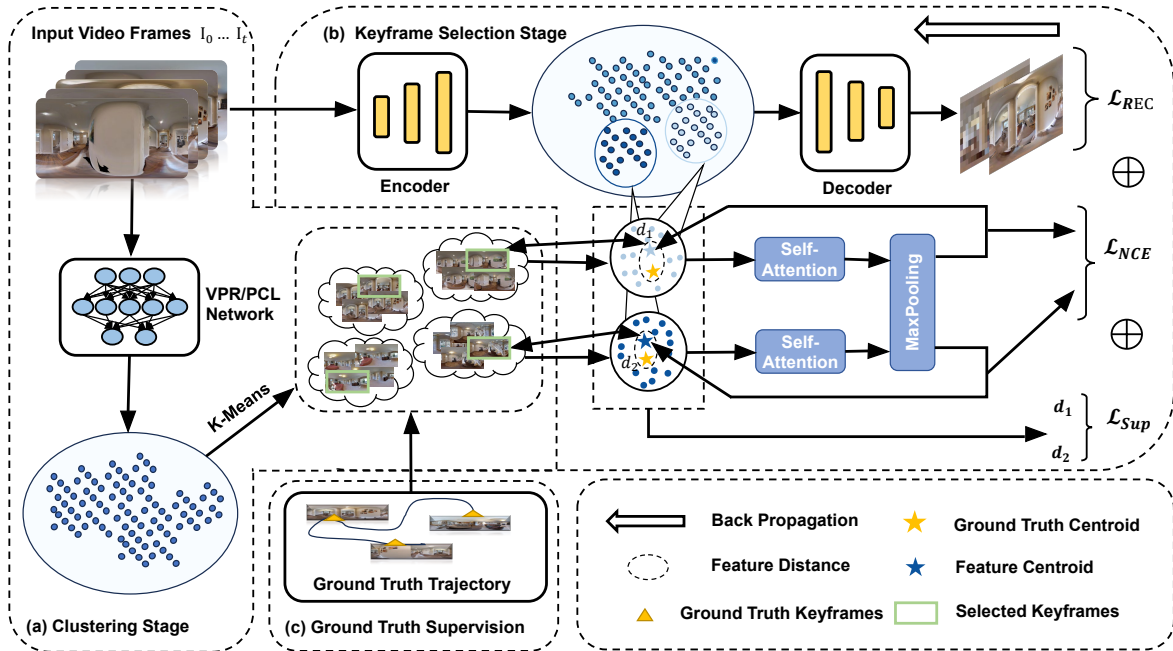


Figure 2. Overview of SceneSum. Clustering and keyframe selection are two major stages in our approach. (1) In clustering stage, We use a PCL/VPR encoder to encode images to feature, then divide all frames into several clusters based on the feature or ground truth odometry if available. In the selection stage, we choose the most representative frame for each cluster, ensuring that each selected frame is visually distinct. Additionally, if spatial information is available in the training set, we have an optional Ground Truth supervision stage. Once enabled, this pipeline is switched from a self-supervised model to a supervised model. Specifically, we use pre-computed keyframes obtained from ground truth trajectory to guide our selection of keyframes. Note that the frames circled in green represent the selected frames

and pose drifting. To address this, Yang *et al.* [46] propose a method where a robot follows a person to capture effective videos around them. However, this approach may not be suitable for empty rooms. This demonstrates the complexities in SLAM-based video summarization.

Clustering. The goal of clustering is to partition a set of data points into distinct groups or clusters. Most video summarization methods [1, 2, 56] utilize clustering to group similar frames together, reducing data complexity, eliminating redundancy, and extracting key scenes for efficient summary generation. In this paper, we select the Prototypical contrastive learning (PCL) [29] and NetVLAD (together with K-Nearest Neighbors (KNN)) [3, 6, 21] for clustering, because of their applications in visual navigation in [7, 28]

3. Scene Summarization

3.1. Problem Formulation

Imagine a mobile agent (*e.g.*, a robot, a self-driving car, *etc.*) equipped with an RGB camera while moving in an environment (either indoor or outdoor). To provide an efficient means for users to grasp essential information, scene summarization is to compress a long series of input images $\mathcal{I} = I_1, I_2, \dots, I_n$ into a small set of keyframes $\mathcal{K} = K_1, K_2, \dots, K_m$ that capture the scene’s essence, where I_i and $K_i \in \mathbb{R}^{H \times W \times 3}$. This setup is similar to the video

summarization setup. However, as discussed in Sec. 3.5, scene summarization concentrates on comprehending spatial scene structure and the evaluation for both tasks differs.

We propose an adaptable neural network summarizer **SceneSum** for scene summarization task, parameterized by ϕ , to generate these keyframes without explicit frame-level importance labels. We are interested in solving this task in two different modes: (1) generalization, and (2) auto-labeling. The goal of (1) refers to a model’s zero-shot summarization performance on data outside the training set, assessing its adaptability to unseen samples. In contrast, the objective of (2) refers to assessing the overfitting performance of a self-supervised model specifically on the training set.

SceneSum is a clustering-based keyframe summarizer network in two modes: (1) self-supervision, and (2) weak supervision utilizing ground truth geo-labels. The difference between these two modes is highlighted in Fig. 2. Overall, as depicted in the figure, the pipeline consists of 2 main stages and 1 optional module: (1) frames clustering, (2) keyframe selection, and (3) ground truth supervision.

3.2. Frames Clustering

Inspired by VSUMM [10], clustering is used to discover patterns, groups, or subsets within a dataset, aiding in preprocessing a large dataset and dividing it into several

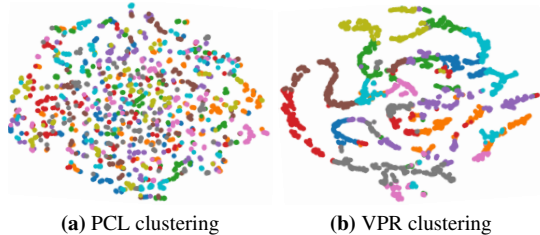


Figure 3. t-SNE plot for PCL and VPR clustering approaches

groups of images, where the images in one group appear more similar to each other than to those in other groups. In this work, we applied three ways of clustering techniques including contrastive-based, visual place recognition-based, and ground truth supervision-based techniques.

Contrastive based clustering. Classic deep learning-based video summarization methods [10, 25] rely on image feature for clustering, such as contrastive-based clustering method prototypical contrastive learning (PCL) [29] and applying K-means on ResNet/VGG features [10]. In this work, we applied PCL as one of the clustering methods, because of its extensive application in visual navigation tasks in [28]. We present a t-SNE plot [42] of PCL clustering from our Habitat-Sim experiment, as illustrated in Fig. 3a. The features appear relatively sparse.

Visual place recognition based clustering. However, we believe that the image feature is not the best choice for scene summarization because it does not encode spatial information. Thus, we also leverage deep learning-based Visual Place Recognition (VPR) features from NetVLAD [6], which is extensively used in SLAM tasks [7, 17, 18]. It aggregates local descriptors into a global representation, making it effective for capturing the overall *visual* content and *spatial* relationships within an image. The feature distribution is depicted in Fig. 3b. Notably, we observe a relatively continuous feature map, resembling the distribution of the actual trajectory.

K-nearest neighbor (KNN). KNN assigns each frame to its nearest cluster based on PCL and NetVLAD feature distance metrics, such as Euclidean distance. As an example, if we target obtaining 5 keyframes for a set of 500 frames sampled from a video, we set $k=5$ and KNN inherently partitions 500 images into 5 clusters with roughly equal sizes.

Ground truth supervision based clustering. In this study, we introduce a ground truth supervision module that transforms our approach from self-supervised to supervised, as shown in Fig. 2. In this scenario, each frame is assigned to its closest cluster based on the Euclidean distance of ground truth poses. The keyframes are then selected as the centroids of these clusters.

Cluster sampling. For computation efficiency and robustness, we only sample equal-sized images from each cluster. Mathematically, let each cluster \mathcal{C}_j represent the set of images within cluster j . Every time we need to retrieve

a cluster of images, we randomly select N images from \mathcal{C}_j , denoted as $\mathcal{S}_j \subset \mathcal{C}_j$.

3.3. Keyframe Selection

After Sec. 3.2, we need to select 1 keyframe within each cluster. Traditional method like VSUMM [10] takes the centroid of each cluster as the keyframe in the feature space. However, the centroid of the clusters in the feature space does not explicitly mean the centroid of clusters in 3D spatial space. Instead, we employed an encoder-decoder structure together with contrastive loss and an optional GT supervision pipeline to help the selected keyframe sets both visually and spatially separate.

Autoencoder. Autoencoders contribute by generating features that provide each image with a refined representation. This intrinsic property ensures that the latent space constructed by the Autoencoder encapsulates the most salient characteristics of the images, facilitating subsequent keyframe selection processes. Given an input image \mathbf{I}_i , an Autoencoder consists of two main components: an encoder function $f(\mathbf{I}_i)$ and a decoder function $g(\mathbf{h})$. The encoder maps the input data to a lower-dimensional latent space representation, denoted as $\mathbf{h} = f(\mathbf{I}_i)$. The decoder then attempts to reconstruct the original data from the encoded representation, yielding a reconstruction $\mathbf{I}_i' = g(\mathbf{h})$.

Pooling layer. The pooling layer reduces a 2D image feature vectors ($N \times D$) of \mathcal{S}_j to a 1D global feature vector $p_j(1 \times D)$, where D is an image feature dimension. Next, we perform a KNN search within \mathcal{C}_j 's feature space by taking p_j as the query. The idea is to select the image whose feature vector with the closest distance to the given global vector p_j in a certain cluster. Thus the image is designated as the keyframe for that particular cluster.

3.4. Loss

The loss function comprises two major components and one option component for ground truth supervision: the reconstruction loss, the InfoNCE loss, and the ground truth supervision loss (optional).

Reconstruction loss. The reconstruction loss involves the utilization of the autoencoder for image representation learning. For each image \mathbf{I}_i , the autoencoder mechanism encompasses encoding and decoding stages, ultimately resulting in the reconstructed image \mathbf{I}_i' . The reconstruction loss $\mathcal{L}_{\text{Recons.}}$ is then defined as the L2 loss between the original and the reconstructed images:

$$\mathcal{L}_{\text{Recons.}} = \frac{1}{N} \sum_{i=1}^N \|\mathbf{I}_i - \mathbf{I}_i'\|_2^2 \quad (1)$$

InfoNCE loss. In addition, the InfoNCE, which stands for Information Noise-Contrastive Estimation loss, plays a crucial role in separating the keyframes from each cluster by

using contrastive-based loss InfoNCE. The InfoNCE principle asserts that the features of every element from any two clusters \mathcal{S}_a and \mathcal{S}_b should serve as negative pairs to each other. Mathematically, the InfoNCE loss between clusters \mathcal{S}_a and \mathcal{S}_b is defined as:

$$\mathcal{L}_{\text{InfoNCE}_{a,b}} = -\log \frac{e^{\text{sim}(\mathbf{p}_a, \mathbf{p}_a)}}{e^{\text{sim}(\mathbf{p}_a, \mathbf{p}_a)} + e^{\text{sim}(\mathbf{p}_a, \mathbf{p}_b)}} \quad (2)$$

where $\text{sim}(\cdot)$ is the similarity function and $e^{\text{sim}(\mathbf{p}_a, \mathbf{p}_b)}$ denotes the exponential of the similarity score between \mathbf{p}_a and \mathbf{p}_b ; \mathbf{p}_a and \mathbf{p}_b are the pooled(global) features of clusters \mathcal{S}_a and \mathcal{S}_b respectively.

Ground truth supervision loss. As previously discussed in Sec. 3.2, the transition from a self-supervised to a supervised approach involves the incorporation of a Ground Truth (GT) supervision module. In the supervised method, apart from the change in clustering strategy, we also introduce the ground truth supervision Loss \mathcal{L}_{GT} as:

$$\mathcal{L}_{\text{GT}} = \frac{1}{N} \sum_{i=1}^N \|f(\mathbf{I}_i^{\text{GT}}) - \mathbf{p}_i\|_2^2, \quad (3)$$

where $f(\cdot)$ is the autoencoder function, \mathbf{I}_i^{GT} is the keyframe selected by the ground truth pose for i -th cluster, \mathbf{p}_i is the pooled global feature for i -th cluster.

Self-supervised vs supervised loss. For our basic self-supervised method, the total self-supervised loss $\mathcal{L}_{\text{self}}$ becomes the sum of the reconstruction loss and the InfoNCE loss across all pairs of clusters as follows:

$$\mathcal{L}_{\text{self}} = \mathcal{L}_{\text{Recons.}} + \sum_{a,b \in \mathcal{S}} \mathcal{L}_{\text{InfoNCE}_{a,b}} \quad (4)$$

Besides, for supervised loss $\mathcal{L}_{\text{supervised}}$, we need to add \mathcal{L}_{GT} to further reduce the gap between the selected frame and the actual cluster centroid from the ground truth pose:

$$\mathcal{L}_{\text{supervised}} = \mathcal{L}_{\text{Recons.}} + \sum_{a,b \in \mathcal{S}} \mathcal{L}_{\text{InfoNCE}_{a,b}} + \mathcal{L}_{\text{Supervision}} \quad (5)$$

3.5. Evaluation Metrics

Different from the video summarization task, our work focuses on the spatial diversity of the selected keyframes. Thus, we introduce a new metric **Divergence** to evaluate the keyframe spatial diversity.

Divergence metric. Suppose the divergence metric D is employed to evaluate the similarity between images within a summarized set. A "similar pair" of images is defined as a pair with Euclidean distances greater than a specified threshold hyperparameter r . Divergence loss penalizes by taking the sum of all similar pairs. The diversity $D \in [0, 1]$ can be summarized as:

$$D = \frac{\sum_{I_i \in \mathcal{K}} |d_i|}{|\mathcal{K}|^2}, \quad (6)$$

$$d_i = \{|I_j| \mid |T(I_i) - T(I_j)| < r, I_j \in \mathcal{K}\} \quad (7)$$

I_i and I_j refer to individual images in the keyframe set \mathcal{K} , $T(\cdot)$ represents the odometry position where the image has been taken, d_i is the size of the similar pair set, r is a distance threshold measured in meter. Methods with a smaller divergence (D) under the same distance threshold (r) are considered superior.

Area under curve. AUC is the area under the divergence curve, where the divergence curve is plotted with *the diversity* on the y-axis and *the distance threshold* r on the x-axis at various thresholds. AUC provides a comprehensive measure of the model's performance across different distance thresholds t , offering a better reflection of the model's classification quality for different classes. Per the divergence metric, lower AUC values represent superior performance.

4. Experiment

Overview. We present a comprehensive exploration of our SceneSum framework, assessing its effectiveness and adaptability in the domain of scene summarization. We conduct thorough analyses on two different datasets: the "Habitat-Sim" simulated indoor panoramic RGB dataset (Sec. 4.2) and the "KITTI" real-world outdoor perspective RGB dataset (Sec. 4.3). We evaluate SceneSum against prominent video summarization methods like PySceneDetect, DR-DSN, CA-SUM, and VSUMM by divergence metric and area-under-curve detailed in Sec. 3.5.

Besides, we also conduct extensive ablation research, delving into a comparative analysis of (1) supervised vs self-supervised method, (2) VPR vs PCL clustering, (3) divergence comparison on different baselines, and (4) auto-labeling capability.

4.1. Experiment Settings

Datasets. We evaluate SceneSum on a simulated RGB dataset using the Habitat-Sim simulator[39] based on the Gibson photorealistic RGB dataset[44]. This dataset comprises panoramic RGB images captured within various indoor scans. To gather RGB images, a panoramic camera mounted on a robot navigated randomly within the virtual environments, resulting in a total of 72,792 RGB images. Each image was subsequently downsampled to dimensions of 512×256 pixels to facilitate processing.

Besides, we also conducted evaluations of SceneSum on outdoor non-panoramic RGB datasets - KITTI [19]. This dataset is recorded by the Point Grey Flea 2 (FL2-14S3C-C) sensor, configured in a roof-mounted pushbroom setup. This dataset comprises 12,483 RGB images covering a driving distance of 73.7 kilometers. After pre-processing, we resize each frame to an image of size 512×256 Each

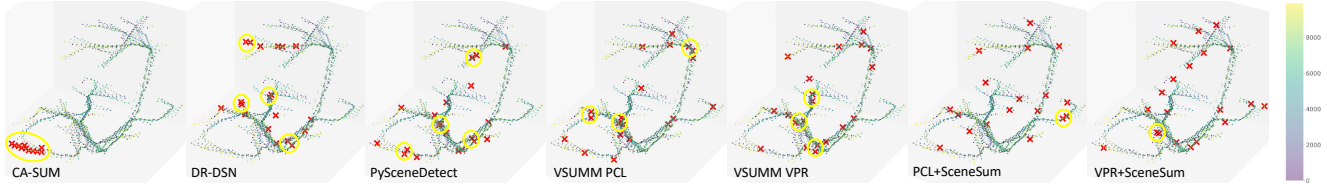


Figure 4. Selected keyframes in Habitat-Sim Dataset. We summarize 20 keyframes of 7 baselines on scene *Stokes*. All frames are color-coded by temporal order. Summarized keyframes are marked with red crosses. Groups of frames that are geographically close to each other are circled in yellow.

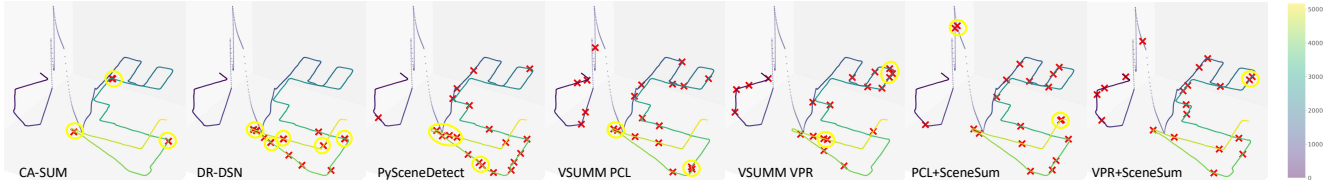


Figure 5. Selected keyframes in KITTI Dataset. We summarize 20 keyframes of 7 baselines on scene *0028*. The baselines and annotations follow Fig. 4

image corresponds to the exact GPS location. Our evaluation focuses on the three most complex scenes within the KITTI dataset, where multiple revisits to various locations occur, and the explored area is considerably vast.

Baseline Methods. The following methods are compared to highlight the effectiveness of the proposed SceneSum. (1) *PySceneDetect*. A classic non-learning approach based on color histograms [36]. (2) *DR-DSN*. [55] and (3) *CA-SUM*. [5] Deep learning-based summarizers. (4) *VSUMM*. A clustering-based video summarizer with PCL and VPR clustering [10]. (5) *SceneSum*. The proposed framework of clustering for summarizing scene video. Our framework has three variants for evaluation: SceneSum with PCL clustering, SceneSum with VPR clustering, and ground truth supervised SceneSum. We use a batch size of 64, a learning rate of 0.001, and an embedding dimension of 2048. The model is trained with the Adam optimizer for 100 epochs.

4.2. Habitat-Sim Experiment

Implementation details. Hyperparameters are investigated, including the distance threshold $r \in [0, 3]$ meters for Habitat-Sim and the size of the targeted keyframe set $k \in \{10, 20, 30, 40\}$. Besides, we selected 6 scenes from the Habitat-Sim dataset for training and testing. We conduct 6 cross-validation experiments on the Habitat-Sim dataset, wherein each experiment involves training the model on five scenes for 100 epochs utilizing the NVIDIA A100 GPU, followed by inference on the remaining scene. In this section, we only focus on self-supervised SceneSum.

Baseline comparisons. In Tab. 1, we evaluated several video summarization methods, including DR-DSN, CA-SUM, PySceneDetect, VSUMM+PCL, and VSUMM+VPR, for the scene summarization task. Among all, CA-SUM underperforms, highlighting its limitations in selecting spatially diverse keyframes. Moreover, VSUMM+PCL and VSUMM+VPR demonstrated nearly

identical, enhanced results in comparison to CA-SUM. Notably, DR-DSN produced performs well when using fewer clusters. Lastly, PySceneDetect emerged as the most effective among all the baselines.

Most significantly, SceneSum outperforms these baselines in terms of the Area Under the Curve (AUC) metric across various cluster sizes, affirming its ability to select more spatially diverse keyframes. Analysis of the data from Tab. 1 reveals that SceneSum significantly outperforms all baselines across six Habitat-Sim scenes. This superiority of SceneSum is further evidenced in Fig. 4, where it typically showcases a more dispersed frame distribution, validating our two-stage model’s efficacy in scene summarization. Improvements were noted across regions and cluster sizes: Micanopy saw a 7.86% increase, Spotswood 42.9%, Springhill 97.6%, Stilwell 82.5%, Stokes 70.1%, and Goffs 45.2%. In cluster analysis, increases were 104% for 10 clusters, 69.9% at 20, 24.0% at 30, and 29.2% at 40.

4.3. KITTI Experiment

Implementation details. The implementation for the KITTI dataset is similar to the one for the Habitat-Sim dataset, with the exception that we modify the distance threshold $r \in [0, 100]$ meters, to accommodate the scalability of the KITTI dataset. Furthermore, we carefully selected three scenes from the KITTI dataset for our training and testing procedures. Referring to our setup in the Habitat-Sim dataset, we also conducted the same cross-validation setup for the KITTI dataset. In this section, we only focus on self-supervised SceneSum.

Baseline comparison. SceneSum performs the best which is especially remarkable considering KITTI’s wide coverage. As indicated in the last two rows of Tab. 2, SceneSum significantly surpasses all baselines which validates the effectiveness of employing a clustering framework for scene summarization. Moreover, Fig. 5 illustrates that akin to Habitat-Sim, the frames in the SceneSum methods ap-

Table 1. Best AUC results for the Habitat-Sim dataset. We conducted experiments under diverse cluster sizes across six scenes, reporting AUC, average (AVG), and standard deviation (SD) values. We emphasize the top three performing baselines using red, teal, and blue highlights respectively, with lower values indicating superior performance.

Scene	Micanopy(↓)						Spotswood(↓)						Springhill(↓)					
	10	20	30	40	AVG.	SD.	10	20	30	40	AVG.	SD.	10	20	30	40	AVG.	SD.
CA-SUM	0.309	0.252	0.254	0.241	0.264	0.031	0.082	0.195	0.206	0.288	0.193	0.085	0.585	0.487	0.357	0.301	0.433	0.128
DR-DSN	0.045	0.172	0.180	0.205	0.151	0.072	0.345	0.457	0.316	0.291	0.352	0.073	0.105	0.240	0.273	0.290	0.227	0.084
VSUMM PCL	0.158	0.218	0.257	0.250	0.221	0.045	0.187	0.234	0.271	0.230	0.230	0.034	0.080	0.179	0.202	0.219	0.170	0.062
VSUMM VPR	0.254	0.324	0.312	0.332	0.306	0.035	0.229	0.321	0.224	0.237	0.253	0.046	0.183	0.141	0.238	0.178	0.185	0.040
PySceneDetect	0.157	0.197	0.172	0.184	0.178	0.017	0.358	0.218	0.218	0.174	0.242	0.080	0.108	0.197	0.207	0.224	0.184	0.052
PCL+SceneSum	0.155	0.152	0.184	0.172	0.166	0.015	0.117	0.151	0.146	0.215	0.171	0.041	0.023	0.086	0.129	0.106	0.086	0.046
VPR+SceneSum	0.118	0.117	0.167	0.159	0.140	0.026	0.067	0.120	0.191	0.163	0.135	0.054	0.101	0.111	0.140	0.138	0.123	0.020

Scene	Stilwell(↓)						Stokes(↓)						Goffs(↓)					
	10	20	30	40	AVG.	SD.	10	20	30	40	AVG.	SD.	10	20	30	40	AVG.	SD.
CA-SUM	0.408	0.543	0.424	0.370	0.436	0.075	1.968	1.791	0.915	0.738	1.353	0.616	0.293	0.190	0.176	0.195	0.214	0.054
DR-DSN	0.176	0.225	0.214	0.222	0.209	0.023	0.206	0.287	0.308	0.344	0.286	0.058	0.059	0.118	0.182	0.181	0.135	0.059
VSUMM PCL	0.272	0.132	0.235	0.214	0.213	0.059	0.117	0.227	0.290	0.248	0.221	0.074	0.104	0.163	0.160	0.173	0.150	0.031
VSUMM VPR	0.107	0.210	0.262	0.250	0.207	0.070	0.267	0.213	0.293	0.290	0.266	0.037	0.080	0.205	0.147	0.183	0.154	0.055
PySceneDetect	0.134	0.260	0.174	0.183	0.188	0.053	0.246	0.235	0.161	0.202	0.211	0.038	0.091	0.181	0.155	0.151	0.145	0.038
PCL+SceneSum	0.093	0.162	0.154	0.147	0.139	0.031	0.094	0.108	0.157	0.193	0.138	0.046	0.073	0.086	0.107	0.112	0.095	0.018
VPR+SceneSum	0.039	0.091	0.130	0.132	0.103	0.044	0.076	0.109	0.158	0.154	0.124	0.039	0.050	0.106	0.096	0.119	0.093	0.030

Scene	Average Result(↓)					
	10	20	30	40	AVG.	SD.
CA-SUM	0.608			0.576		0.389
DR-DSN	0.156			0.250		0.246
VSUMM PCL	0.153			0.192		0.236
VSUMM VPR	0.187			0.236		0.246
PySceneDetect	0.182			0.215		0.181
PCL+SceneSum	0.093			0.124		0.146
VPR+SceneSum	0.075			0.113		0.147

Table 2. Best AUC results for the KITTI dataset. We conduct experiments across three scenes. All other setup and abbreviations follow Tab. 1

Scene	KITTI (0018)(↓)						KITTI (0027)(↓)					
	10	20	30	40	AVG.	SD.	10	20	30	40	AVG.	SD.
CA-SUM	98.155	69.287	52.288	42.290	65.505	24.454	49.733	47.028	50.103	44.141	47.751	2.77
DR-DSN	95.678	46.136	23.504	24.485	47.450	33.806	17.777	14.442	13.139	14.793	15.037	1.960
VSUMM PCL	11.155	7.297	6.564	10.566	8.895	2.301	4.288	3.502	3.409	4.562	3.940	0.572
VSUMM VPR	9.166	7.85	8.394	9.591	8.750	0.778	4.355	5.076	6.414	6.037	5.470	0.933
PySceneDetect	5.411	6.015	6.700	8.113	6.559	1.162	2.911	2.939	3.596	4.691	3.534	0.834
PCL+SceneSum	8.955	6.078	7.181	6.866	7.270	1.215	0.655	4.434	2.980	4.717	3.196	1.857
VPR+SceneSum	2.533	4.703	5.688	6.606	4.883	1.748	0.456	1.626	3.094	3.831	2.623	1.508

Scene	KITTI (0028)(↓)						Average Result(↓)					
	10	20	30	40	AVG.	SD.	10	20	30	40	AVG.	SD.
CA-SUM	20.922	56.407	41.347	31.895	37.642	15.038	56.270	57.574	47.913	39.442	50.300	8.409
DR-DSN	10.399	10.915	11.565	12.444	11.330	0.882	41.285	23.831	16.069	17.241	24.606	11.632
VSUMM PCL	0.388	2.342	2.951	3.056	2.184	1.238	5.277	4.380	4.308	6.061	5.007	0.830
VSUMM VPR	3.177	3.305	3.235	3.039	3.189	0.113	5.566	5.410	6.014	6.222	5.803	0.379
PySceneDetect	0.766	3.539	3.194	3.660	2.789	1.364	3.029	4.164	4.496	5.488	4.294	1.014
PCL+SceneSum	0.005	1.736	2.650	2.508	1.926	1.215	3.205	4.083	4.270	4.697	4.064	0.628
VPR+SceneSum	0.000	1.231	1.480	2.321	1.391	0.960	0.996	2.520	3.421	4.253	2.798	1.394

plied to the KITTI dataset exhibit a widespread distribution. Our method SceneSum significantly surpasses all baselines, with AUC improvements of at least 34.3%, 34.7%, and 66.7% in three different scenes.

4.4. Ablation Study

Supervised vs Self-supervised. The purpose of the ablation study in this part of the section is to examine whether the introduction of this supervision loss leads to significant performance differences in the model. Fig. 6 shows the average performance of the supervised and self-supervised methods on Habitat-Sim and KITTI environment. In Fig. 6,

six scenarios are depicted where the comparative performance of the two models is analyzed at Number of Clusters = 10, 20, 30, and 40, using the AUC metric. In the majority of cases, the supervised model slightly outperforms the self-supervised model. Notably, when the number of clusters is set to 10, the supervised technique outperforms the unsupervised method significantly. We demonstrate that introducing ground truth in the training process slightly improves the predictive performance of our framework. However, the gap between supervised SceneSum and self-supervised SceneSum is not substantial. This observation underscores the robustness and effectiveness of self-supervised SceneSum

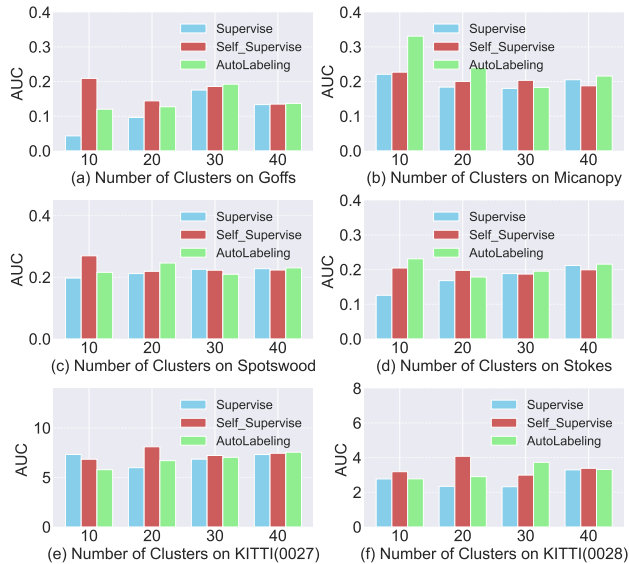


Figure 6. Performance Analysis of Supervised Method, Self-Supervised Method and AutoLabeling under Different Number of Clusters in (a) Goffs (b) Micanopy (c) Spotswood (d) Springhill (e) KITTI(0027) (f) KITTI(0028)

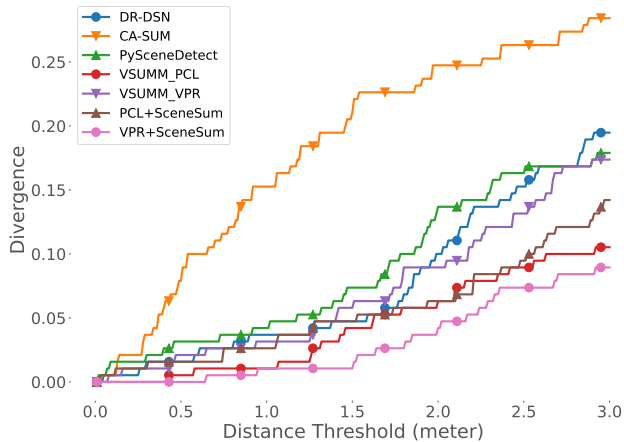


Figure 7. Habitat-Sim (Stillwell) Divergence vs Distance Threshold (meter) at 20 Summarized Frames

across diverse contexts, establishing it as a highly flexible tool in fields where ground truth data may not be available.

VPR vs PCL clustering comparison. Tab. 1 and Tab. 2 indicate that the SceneSum method when coupled with VPR-based clustering, outperforms the PCL-based clustering method significantly in most scenes. This is attributed to the fact that the VPR method captures distinctive information about locations or places, emphasizing scene context, and spatial relationships. This feature is deemed more suitable for scene summarization when contrasted with the PCL method, which captures visual information exclusively.

Divergence comparisons. Fig. 7 and 8 reveal a noteworthy trend in the performance of SceneSum approaches for scene summarization. As the distance threshold increases,

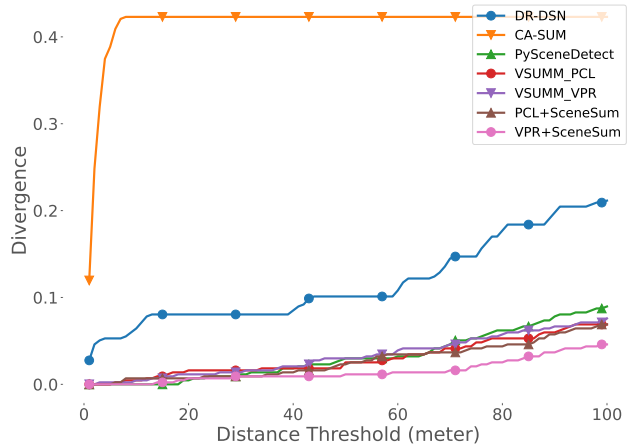


Figure 8. KITTI (0028) Divergence vs Distance Threshold (meter) at 30 Summarized Frames.

there is a corresponding rise in the divergence for all methods. VPR+SceneSum outperforms all baseline methods at all distance thresholds, demonstrating its stable performance regardless of the distance we evaluate.

4.5. Auto-labeling Capability.

Sec. 4.2, 4.3, and 4.4 reveal a key finding that self-supervised SceneSum demonstrates strong summarization performance when zeroshot to a new scene. In this section, we want to investigate the auto-labeling capability of the model. If we do not care about the time taken for scene summarization, we can use SceneSum as a network summarizer to summarize the scene video while training from it.

From Fig. 6, we can observe that auto-labeling outcomes are closely aligned with those of the self-supervised approach. This reverse proves the self-supervised inference capability. Even if we compare self-supervised SceneSum with SceneSum which overfits the test dataset by training from it, the results are similar.

5. Conclusion

In this study, we present a new task - scene summarization, and develop a two-stage supervised or self-supervised approach to scene summarization, leveraging a combination of autoencoder, contrastive learning, and ground truth supervision. This integration has proven highly effective in enhancing the quality of selected keyframes. Furthermore, we tackle the challenge of scene summarization and demonstrate that the incorporation of Visual Place Recognition (VPR) techniques in the cluster acquisition process leads to significantly improved results compared to using the contrastive-based clustering method.

References

- [1] Laith Mohammad Abualigah, Ahamad Tajudin Khader, and Essam Said Hanandeh. Hybrid clustering analysis using improved krill herd algorithm. *Applied Intelligence*, 48:4047–4071, 2018. 3
- [2] Laith Mohammad Abualigah, Ahamad Tajudin Khader, and Essam Said Hanandeh. A new feature selection method to improve the document clustering using particle swarm optimization algorithm. *Journal of Computational Science*, 25: 456–466, 2018. 3
- [3] Amar Ali-Bey, Brahim Chaib-Draa, and Philippe Giguere. Mixvpr: Feature mixing for visual place recognition. In *Proceedings of the IEEE/CVF Winter Conference on A CV*, pages 2998–3007, 2023. 3
- [4] Evlampios Apostolidis, Eleni Adamantidou, Alexandros I Metsai, Vasileios Mezaris, and Ioannis Patras. Ac-sum-gan: Connecting actor-critic and generative adversarial networks for unsupervised video summarization. *IEEE Transactions on Circuits and Systems for Video Technology*, 31(8):3278–3292, 2020. 2
- [5] Evlampios Apostolidis, Georgios Balaouras, Vasileios Mezaris, and Ioannis Patras. Summarizing videos using concentrated attention and considering the uniqueness and diversity of the video frames. In *Proceedings of the 2022 Intl. Conf. on Multimedia Retrieval*, pages 407–415, 2022. 1, 2, 6
- [6] Relja Arandjelovic, Petr Gronat, Akihiko Torii, Tomas Pajdla, and Josef Sivic. Netvlad: Cnn architecture for weakly supervised place recognition. In *Proceedings of the IEEE conference on computer vision and pattern recognition*, pages 5297–5307, 2016. 3, 4
- [7] Chao Chen, Xinhao Liu, Yiming Li, Li Ding, and Chen Feng. Deepmapping2: Self-supervised large-scale lidar map optimization. In *Proceedings of the IEEE/CVF Conference on CVPR*, pages 9306–9316, 2023. 3, 4
- [8] Wei-Ta Chu and Yu-Hsin Liu. Spatiotemporal modeling and label distribution learning for video summarization. In *2019 IEEE 21st International Workshop on Multimedia Signal Processing (MMSp)*, pages 1–6. IEEE, 2019. 2
- [9] Arun Das and Steven L Waslander. Entropy based keyframe selection for multi-camera visual slam. In *2015 IEEE/RSJ International Conference on IROS*, pages 3676–3681. IEEE, 2015. 2
- [10] Sandra Eliza Fontes De Avila, Ana Paula Brandao Lopes, Antonio da Luz Jr, and Arnaldo de Albuquerque Araújo. Vsumm: A mechanism designed to produce static video summaries and a novel evaluation method. *Pattern recognition letters*, 32(1):56–68, 2011. 2, 3, 4, 6
- [11] Anastasios D Doulamis, Nikolaos D Doulamis, and Stefanos D Kollias. A fuzzy video content representation for video summarization and content-based retrieval. *Signal processing*, 80(6):1049–1067, 2000. 2
- [12] Naveed Ejaz, Tayyab Bin Tariq, and Sung Wook Baik. Adaptive key frame extraction for video summarization using an aggregation mechanism. *Journal of Visual Communication and Image Representation*, 23(7):1031–1040, 2012. 2
- [13] Mohamed Elfeki and Ali Borji. Video summarization via actionness ranking. In *2019 IEEE Winter Conference on Applications of Computer Vision (WACV)*, pages 754–763. IEEE, 2019. 2
- [14] Ehsan Elhamifar, Guillermo Sapiro, and Rene Vidal. See all by looking at a few: Sparse modeling for finding representative objects. In *2012 IEEE conference on computer vision and pattern recognition*, pages 1600–1607. IEEE, 2012. 2
- [15] Jiri Fajtl, Hajar Sadeghi Sokeh, Vasileios Argyriou, Dorothy Monekosso, and Paolo Remagnino. Summarizing videos with attention. In *Computer Vision—ACCV 2018 Workshops: 14th Asian Conference on Computer Vision, Perth, Australia, December 2–6, 2018, Revised Selected Papers 14*, pages 39–54. Springer, 2019. 2
- [16] Marco Furini, Filippo Geraci, Manuela Montangero, and Marco Pellegrini. Stimo: Still and moving video storyboard for the web scenario. *Multimedia Tools Appl.*, 46(1):47–69, 2010. 2
- [17] Sourav Garg and Michael Milford. Seqnet: Learning descriptors for sequence-based hierarchical place recognition. *IEEE RAL*, 6(3):4305–4312, 2021. 4
- [18] Sourav Garg, Madhu Vankadari, and Michael Milford. Seqmatchnet: Contrastive learning with sequence matching for place recognition & relocalization. In *Conference on Robot Learning*, pages 429–443. PMLR, 2022. 4
- [19] Andreas Geiger, Philip Lenz, Christoph Stiller, and Raquel Urtasun. Vision meets robotics: The kitti dataset. *International Journal of Robotics Research (IJRR)*, 2013. 5
- [20] Ciocca Gianluigi and Schettini Raimondo. An innovative algorithm for key frame extraction in video summarization. *Journal of Real-Time Image Processing*, 1:69–88, 2006. 2
- [21] Stephen Hausler, Sourav Garg, Ming Xu, Michael Milford, and Tobias Fischer. Patch-netvlad: Multi-scale fusion of locally-global descriptors for place recognition. In *Proceedings of the IEEE/CVF Conference on CVPR*, pages 14141–14152, 2021. 3
- [22] Cheng Huang and Hongmei Wang. A novel key-frames selection framework for comprehensive video summarization. *IEEE Transactions on Circuits and Systems for Video Technology*, 30(2):577–589, 2019. 2
- [23] Zhong Ji, Kailin Xiong, Yanwei Pang, and Xuelong Li. Video summarization with attention-based encoder-decoder networks. *IEEE Transactions on Circuits and Systems for Video Technology*, 30(6):1709–1717, 2019. 2
- [24] Zhong Ji, Fang Jiao, Yanwei Pang, and Ling Shao. Deep attentive and semantic preserving video summarization. *Neurocomputing*, 405:200–207, 2020. 2
- [25] Richard M Jiang, Abdul H Sadka, and Danny Crookes. Advances in video summarization and skimming. In *Recent advances in multimedia signal processing and communications*, pages 27–50. Springer, 2009. 4
- [26] Yunjae Jung, Donghyeon Cho, Dahun Kim, Sanghyun Woo, and In So Kweon. Discriminative feature learning for unsupervised video summarization. In *Proceedings of the AAAI Conference on artificial intelligence*, pages 8537–8544, 2019. 2
- [27] Yunjae Jung, Donghyeon Cho, Sanghyun Woo, and In Kweon. Global-and-local relative position embedding for unsupervised video summarization. *ECCV*, pages 167–183, 2020. 2

- [28] Obin Kwon, Nuri Kim, Yunho Choi, Hwiyeon Yoo, Jeongho Park, and Songhwa Oh. Visual graph memory with unsupervised representation for visual navigation. In *Proceedings of the IEEE/CVF International Conference on Computer Vision*, pages 15890–15899, 2021. 3, 4
- [29] Junnan Li, Pan Zhou, Caiming Xiong, and Steven CH Hoi. Prototypical contrastive learning of unsupervised representations. *arXiv preprint arXiv:2005.04966*, 2020. 3, 4
- [30] Ping Li, Qinghao Ye, Luming Zhang, Li Yuan, Xianghua Xu, and Ling Shao. Exploring global diverse attention via pairwise temporal relation for video summarization. *Pattern Recognition*, 111:107677, 2021. 2
- [31] Buyun Liang, Na Li, Zheng He, Zhongyuan Wang, Youming Fu, and Tao Lu. News video summarization combining surf and color histogram features. *Entropy*, 23(8):982, 2021. 2
- [32] Xiaohu Lin, Fuhong Wang, Lei Guo, and Wanwei Zhang. An automatic key-frame selection method for monocular visual odometry of ground vehicle. *IEEE Access*, 7:70742–70754, 2019. 2
- [33] Yen-Ting Liu, Yu-Jhe Li, Fu-En Yang, Shang-Fu Chen, and Yu-Chiang Frank Wang. Learning hierarchical self-attention for video summarization. In *2019 IEEE international conference on image processing (ICIP)*, pages 3377–3381. IEEE, 2019. 2
- [34] Behrooz Mahasseni, Michael Lam, and Sinisa Todorovic. Unsupervised video summarization with adversarial lstm networks. *CVPR*, pages 2982–2991, 2017. 2
- [35] Padmavathi Mundur, Yong Rao, and Yelena Yesha. Keyframe-based video summarization using Delaunay clustering. *International Journal on Digital Libraries*, 6(2):219–232, 2006. 2
- [36] Zachary N. J. Peterson and Brendon J. Brewer. pyscenedetect: An open source scene detection implementation in python. *Journal of Open Source Software*, 2(10):182, 2017. 1, 6
- [37] Mrigank Rochan and Yang Wang. Video summarization by learning from unpaired data. In *Proceedings of the IEEE/CVF Conference on Computer Vision and Pattern Recognition*, pages 7902–7911, 2019. 2
- [38] Mrigank Rochan, Linwei Ye, and Yang Wang. Video summarization using fully convolutional sequence networks. *ECCV*, pages 358–374, 2018. 2
- [39] Manolis Savva, Abhishek Kadian, Oleksandr Maksymets, Yili Zhao, Erik Wijmans, Bhavana Jain, Julian Straub, Jia Liu, Vladlen Koltun, Jitendra Malik, et al. Habitat: A platform for embodied AI research. In *ICCV*, 2019. 5
- [40] Manasa Srinivas, MM Manohara Pai, and Radhika M Pai. An improved algorithm for video summarization—a rank based approach. *Procedia Computer Science*, 89:812–819, 2016. 2
- [41] John Stalbaum and Jae-bok Song. Keyframe and inlier selection for visual slam. In *2013 10th International Conference on URAI*, pages 391–396. IEEE, 2013. 2
- [42] Laurens Van der Maaten and Geoffrey Hinton. Visualizing data using t-sne. *Journal of machine learning research*, 9(11), 2008. 4
- [43] Jiaxin Wu, Sheng-hua Zhong, Jianmin Jiang, and Yunyun Yang. A novel clustering method for static video summarization. *Multimedia Tools and Applications*, 76:9625–9641, 2017. 2
- [44] Fei Xia, Amir R. Zamir, Zhi-Yang He, Alexander Sax, Jitendra Malik, and Silvio Savarese. Gibson env: real-world perception for embodied agents. In *CVPR*, 2018. 5
- [45] Gokhan Yaliniz and Nazli Ikizler-Cinbis. Using independently recurrent networks for reinforcement learning based unsupervised video summarization. *Multimedia Tools and Applications*, 80:17827–17847, 2021. 2
- [46] Chih-Yuan Yang, Heeseung Yun, Srenavis Varadaraj, and Jane Yung-jen Hsu. Acm. In *A Mobile Robot Generating Video Summaries of Seniors’ Indoor Activities*, New York, NY, USA, 2019. Association for Computing Machinery. 2, 3
- [47] Huan Yang, Baoyuan Wang, Stephen Lin, David P. Wipf, Minyi Guo, and Baining Guo. Unsupervised extraction of video highlights via robust recurrent auto-encoders. *CoRR*, abs/1510.01442, 2015. 2
- [48] Li Yuan, Francis EH Tay, Ping Li, Li Zhou, and Jiashi Feng. Cycle-sum: Cycle-consistent adversarial lstm networks for unsupervised video summarization. In *Proceedings of the AAAI Conference on Artificial Intelligence*, pages 9143–9150, 2019. 2
- [49] Ke Zhang, Wei-Lun Chao, Fei Sha, and Kristen Grauman. Video summarization with long short-term memory. In *Computer Vision—ECCV 2016: 14th European Conference, Amsterdam, The Netherlands, October 11–14, 2016, Proceedings, Part VII 14*, pages 766–782. Springer, 2016. 2
- [50] Ying Zhang, Guanfeng Wang, Beomjoo Seo, and Roger Zimmermann. 3rd multimedia systems conference. In *Multi-Video Summary and Skim Generation of Sensor-Rich Videos in Geo-Space*, page 53–64, New York, NY, USA, 2012. Association for Computing Machinery. 2
- [51] Yujia Zhang, Xiaodan Liang, Dingwen Zhang, Min Tan, and Eric P. Xing. Unsupervised object-level video summarization with online motion auto-encoder. *CoRR*, abs/1801.00543, 2018. 2
- [52] Yujia Zhang, Xiaodan Liang, Dingwen Zhang, Min Tan, and Eric P Xing. Unsupervised object-level video summarization with online motion auto-encoder. *Pattern Recognition Letters*, 130:376–385, 2020. 2
- [53] Bin Zhao, Xuelong Li, and Xiaoqiang Lu. Hsa-rnn: Hierarchical structure-adaptive rnn for video summarization. In *Proceedings of the IEEE conference on computer vision and pattern recognition*, pages 7405–7414, 2018. 2
- [54] Bin Zhao, Xuelong Li, and Xiaoqiang Lu. Property-constrained dual learning for video summarization. *IEEE transactions on neural networks and learning systems*, 31(10):3989–4000, 2019. 2
- [55] Kaiyang Zhou, Yu Qiao, and Tao Xiang. Deep reinforcement learning for unsupervised video summarization with diversity-representativeness reward. In *Proceedings of the AAAI Conf. on Artificial Intelligence*, 2018. 1, 2, 6
- [56] Yongquan Zhou, Haizhou Wu, Qifang Luo, and Mohamed Abdel-Baset. Automatic data clustering using nature-inspired symbiotic organism search algorithm. *Knowledge-Based Systems*, 163:546–557, 2019. 3

Supplementary

This supplement contains more ablation studies, time complexities, and visualizations that could not fit in the study. In particular, we include (1) extra examples on divergence vs distance threshold, (2) time complexity for different methods, (3) discussions on SLAM methods, and (4) more visualizations of selected keyframes.

A. Extra examples on divergence vs distance threshold

We present additional examples comparing divergence versus distance threshold, comprising 4 examples on Habitat-Sim and 3 examples on KITTI. Overall, this follows the previous experiments conducted in Table I and Table II, where VPR+SceneSum demonstrated the best results, followed by PCL+SceneSum.

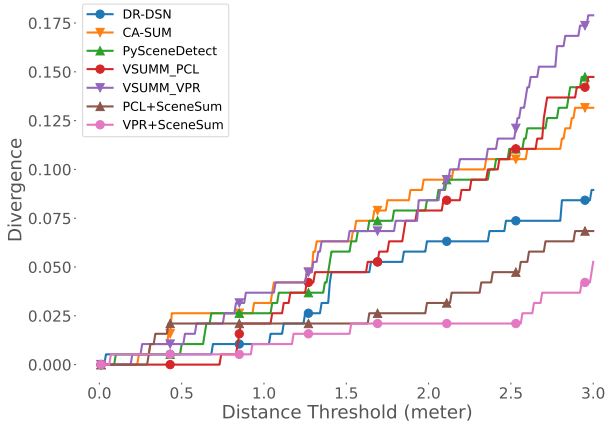


Figure I. Habitat-Sim (Goffs) Divergence vs Distance Threshold (meter) at 20 Summarized Frames

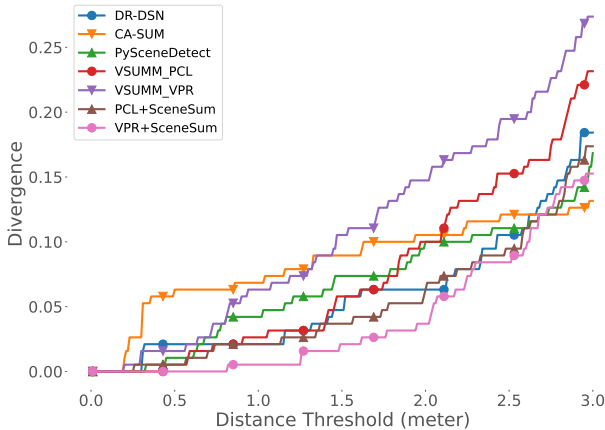


Figure II. Habitat-Sim (Micanopy) Divergence vs Distance Threshold (meter) at 20 Summarized Frames

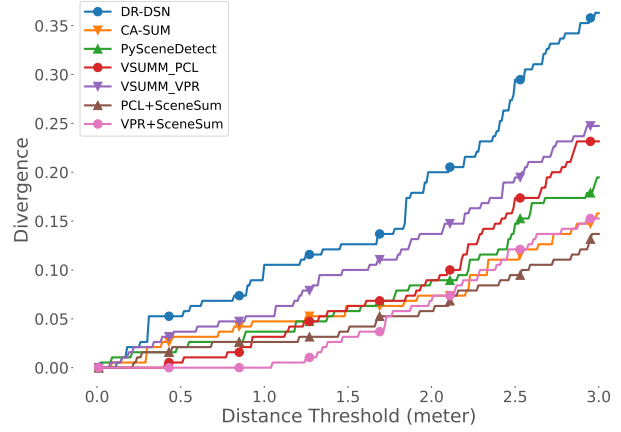


Figure III. Habitat-Sim (Spotswood) Divergence vs Distance Threshold (meter) at 20 Summarized Frames

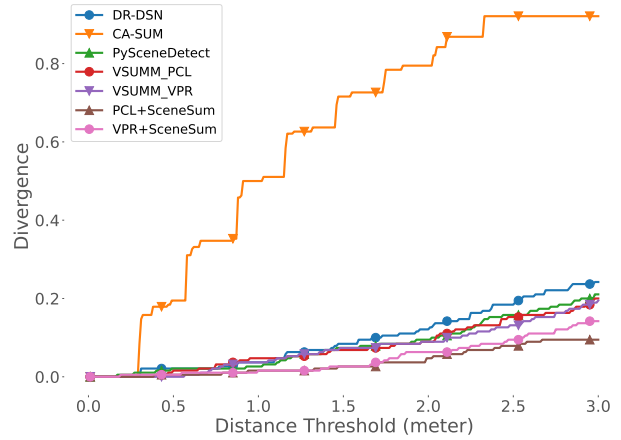


Figure IV. Habitat-Sim (Stokes) Divergence vs Distance Threshold (meter) at 20 Summarized Frames

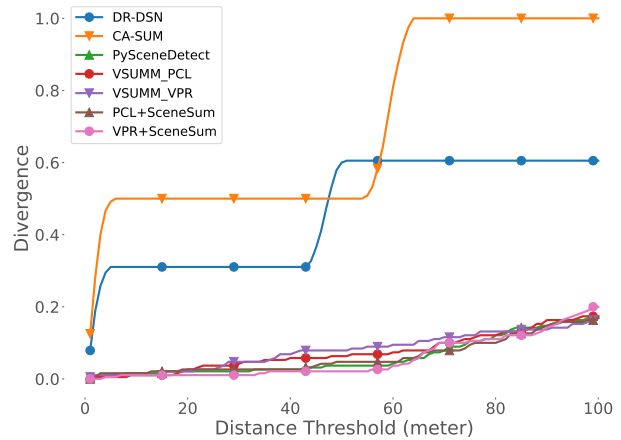


Figure V. KITTI (0018) Divergence vs Distance Threshold (meter) at 20 Summarized Frames

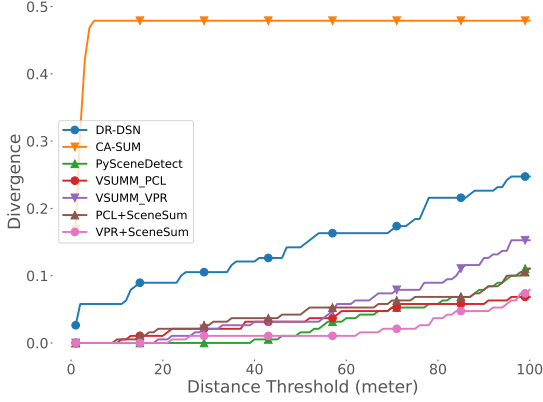


Figure VI(a). KITTl (0027) Divergence vs Distance Threshold (meter) at 20 Summarized Frames

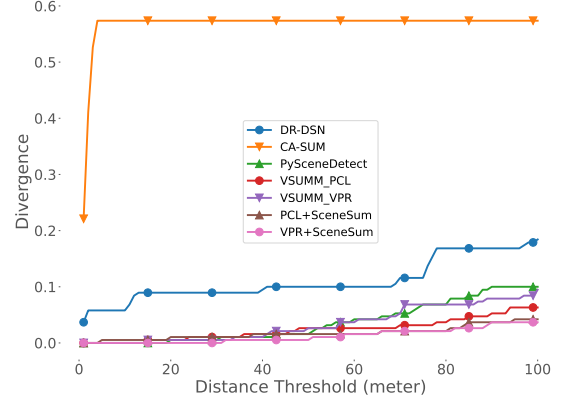


Figure VI(b). KITTl (0028) Divergence vs Distance Threshold (meter) at 20 Summarized Frames

B. Time complexity for different methods

We have included the time taken by both the baseline methods and our approach in Table. I and Table. II. For non-machine learning-based methods, self-supervised, and supervised methods, we only consider the inference time for the test set. However, for autolabelling, we include the training time as part of the overall time calculation, because for autolabelling, training is an integral component of the optimization process.

Table I. Inference Time (seconds) for Habitat-Sim Dataset. (s) represents the methods supervised by ground truth. (a) represents the methods with autolabelling.

Scene	Goffs	Micanopy	Spotswood	Springhill	Stilwell	Stokes
DR-DSN	63.376	27.983	30.089	37.623	38.099	22.257
CA-SUM	139.969	51.596	51.098	64.564	67.103	46.769
PySceneDetect	17.563	6.764	7.516	9.484	10.809	6.074
VSUMM VPR	23.475	8.893	9.211	11.409	13.39	6.496
VSUMM PCL	20.03	9.702	9.85	13.002	12.156	7.713
VPR+SceneSum	183.305	206.311	89.960	293.312	97.829	64.503
PCL+SceneSum	166.037	207.957	75.142	292.857	95.879	56.893
VPR+SceneSum(S)	194.999	166.694	128.187	383.043	95.815	58.244
PCL+SceneSum(S)	185.233	172.785	147.617	394.343	84.859	60.510
VPR+SceneSum(A)	148.894	149.157	81.360	304.567	78.026	54.432
PCL+SceneSum(A)	151.797	138.924	74.393	309.289	75.936	57.571

Table II. Inference Time (seconds) for KITTl Dataset. Table caption follows by Table. I

Scene	KITTl(0018)	KITTl(0027)	KITTl(0028)
DR-DSN	16.775	16.017	18.354
CA-SUM	52.493	34.428	43.639
PySceneDetect	1.92	4.015	4.48
VSUMM VPR	1.78	3.098	3.461
VSUMM PCL	1.462	2.432	2.898
VPR+SceneSum	26.395	43.996	60.562
PCL+SceneSum	22.730	37.828	56.860
VPR+Supervised	19.084	38.316	56.531
PCL+Supervised	18.183	34.909	52.305
VPR+Autolabelling	17.350	34.002	50.562
PCL+Autolabelling	17.442	33.426	46.654

C. Discussions on SLAM methods

People might be concerned that SLAM+KNNN can easily solve this problem. However, attempts to map the entire scene using SLAM methods such as OpenVSLAM were unsuccessful within Habitat sceneries at a sampling rate of 1 frame per second. Our study encountered a significant challenge during the mapping process using openVSLAM. Specifically, OpenVSLAM experienced a loss of tracking, resulting in the failure to generate a complete map as illustrated in Figure. VII

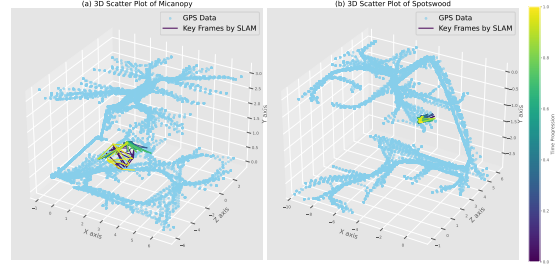


Figure VII. OpenVSLAM fails to create a complete map in Scene Micanopy and Spotswood

We observed a persistent issue with our SLAM (Simultaneous Localization and Mapping) methodology, where it consistently loses track during the map generation phase. This recurring problem leads to the production of maps that are ultimately disorganized and unstructured. This highlights a fundamental limitation in our current SLAM approach, necessitating further investigation and improvement to achieve reliable and orderly map generation.

D. More visualizations on selected keyframes

We have presented more visualizations on selected keyframes, including 5 Habitat scenes and 2 KITTl scenes, as shown in Figure. VIII, Figure. IX, Figure. X, Figure. XI, Figure. XII, Figure. XIII, and Figure. XIV.

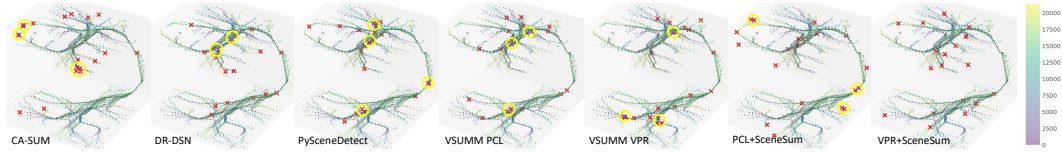


Figure VIII. Selected keyframes in Habitat-Sim Dataset. We summarize 20 keyframes of 7 baselines on scene *Goffs*. All frames are color-coded by temporal order. Summarized keyframes are marked with red crosses. Groups of frames that are geographically close to each other are circled in yellow.

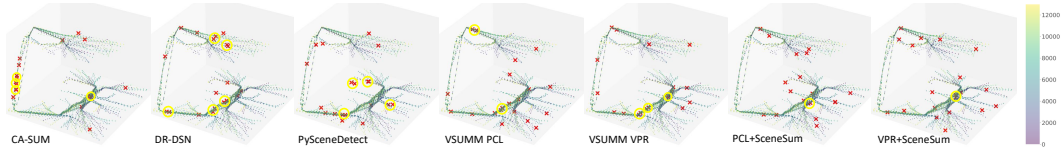


Figure IX. Selected keyframes in Habitat-Sim Dataset. We summarize 20 keyframes of 7 baselines on scene *Stilwell*. The baselines and annotations follow Fig. VIII

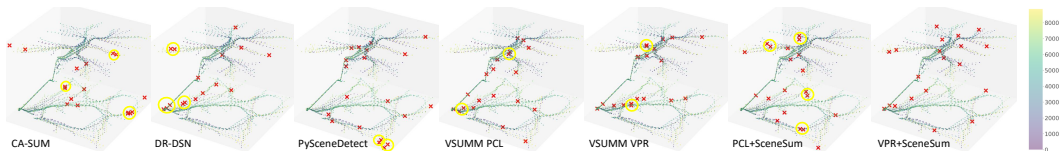


Figure X. Selected keyframes in Habitat-Sim Dataset. We summarize 20 keyframes of 7 baselines on scene *Micanopy*. The baselines and annotations follow Fig. VIII

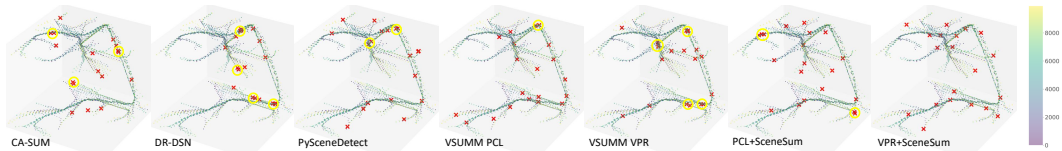


Figure XI. Selected keyframes in Habitat-Sim Dataset. We summarize 20 keyframes of 7 baselines on scene *Spotswood*. The baselines and annotations follow Fig. VIII

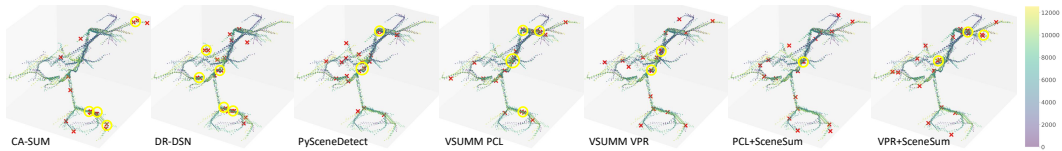


Figure XII. Selected keyframes in Habitat-Sim Dataset. We summarize 20 keyframes of 7 baselines on scene *Springhill*. The baselines and annotations follow Fig. VIII

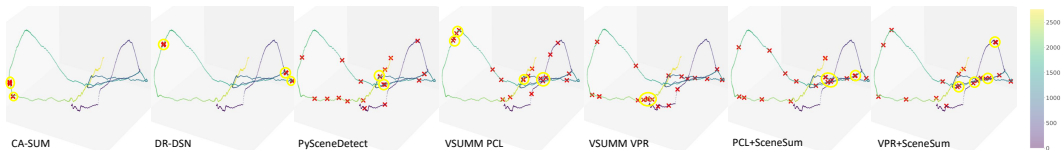


Figure XIII. Selected keyframes in KITTI Dataset. We summarize 20 keyframes of 7 baselines on scene *0018*. The baselines and annotations follow Fig. VIII

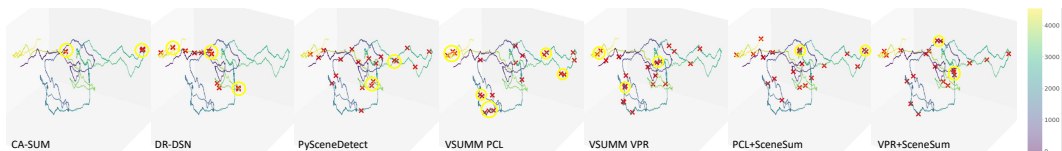


Figure XIV. Selected keyframes in KITTI Dataset. We summarize 20 keyframes of 7 baselines on scene *0027*. The baselines and annotations follow Fig. VIII